CrossMark

Spatial variations of the crustal stress field in the Philippine region from inversion of earthquake focal mechanisms and their tectonic implications

Wen-Nan Wu [a,c], Chung-Liang Lo [b], Jing-Yi Lin [b,c,*]

[a] *Institute of Earth Sciences, Academia Sinica, No. 128, Sec. 2, Academia Road, Nangang Dist., Taipei 11529, Taiwan*
[b] *Department of Earth Sciences, National Central University, 300 Jhongda Road, Jhongli Dist., Taoyuan City 32001, Taiwan*
[c] *Center for Environmental Studies, National Central University, 300 Jhongda Road, Jhongli Dist., Taoyuan City 32001, Taiwan*

ARTICLE INFO

ABSTRACT

This paper presents the spatial variations in the crustal stress field for the Philippine region. Based on the stress configuration, we divided the stress regime in the area of the Philippines into four parts: (1) Trench-perpendicular compressive stress axes (σ_1) with an intermediate plunge were observed along the eastern subduction systems of the Philippine Mobile Belt (PMB), which suggests that the subduction of the Philippine Sea Plate (PSP) is the primary factor controlling the stress distribution. (2) Characterized by systematically rotated σ_1 with very shallow plunge, the central-western portion of the Philippines appears to be largely affected by the collision between the Palawan Block and the PMB. (3) The σ_1 distribution in the northern part of Luzon Island (north of 14°N) is compatible with the plate motion of the PSP, whereas the extensional axes (σ_3) has a fan-shaped stress signature with N-S direction at the south and a more spreading direction to the north, which implies its north escapement. (4) Bounded by the Scarborough Seamount, the northern and southern portions of the Manila Trench reveal a very distinct stress pattern with a trench-parallel σ_3 to the north and a trench-perpendicular σ_3 to the south. This observation may infer a potential effect caused by the presence of the oceanic bathymetric highs on the behavior of the subduction process. In addition to the identification of the four provinces with different stress regimes, we suggest that the Philippine Fault Zone may play an important role to alter the stress state in the region of the Philippines.

© 2017 Elsevier Ltd. All rights reserved.

1. Introduction

The tectonic setting of the Philippines is complex, as the region is mostly surrounded by two subduction zones with nearly opposite orientations. Offshore the eastern Philippines, the Philippine Sea Plate (PSP) subducts westward beneath the Philippine Islands along the Eastern Luzon Trough-Philippine Trench. In the western Philippines, the Sunda Slab subducts eastward along the Manila–Negros–Cotabato Trenches. Across the Philippines, the relative plate motion between the Sunda Block (SB) and the PSP is directed 294°N on average and has an estimated rate of more than 95 mm/yr based on the recent global plate motion model, the NNR-MORVEL56 model (Argus et al., 2011) (Fig. 1). This global

plate motion model refines the precision and accuracy of the geometric and kinematic parameters for 56 plates that are partly taken from an updated digital model of plate boundaries by Bird (2003). Meanwhile, the latest GPS measurements (between 1996 and 2008) show that the station velocities in the Taiwan-Luzon region with respect to the Sunda Block are about 49–89 mm/year in the WNW to NW direction (Yu et al., 2013). It is noticeable that previous studies have exposed that there are significant decreases in GPS velocities from north to south Luzon (Rangin et al., 1999; Hsu et al., 2012). This is incompatible with the prediction generated by the theoretical plate motion model, and implies that the Luzon region may be an independent elastic block (Rangin et al., 1999). Regardless of the tectonic complexity, the high plate convergence rate leads to numerous earthquakes. In particular, 19 large crustal ($\leq$40 km) earthquakes of Mw $\geq$ 7 were reported in the Philippines from 1 January 1976 to 31 July 2015 based on the global Centroid Moment Tensor (GCMT) catalog (Dziewonski et al., 1981) (http://www.globalcmt.org, last accessed November
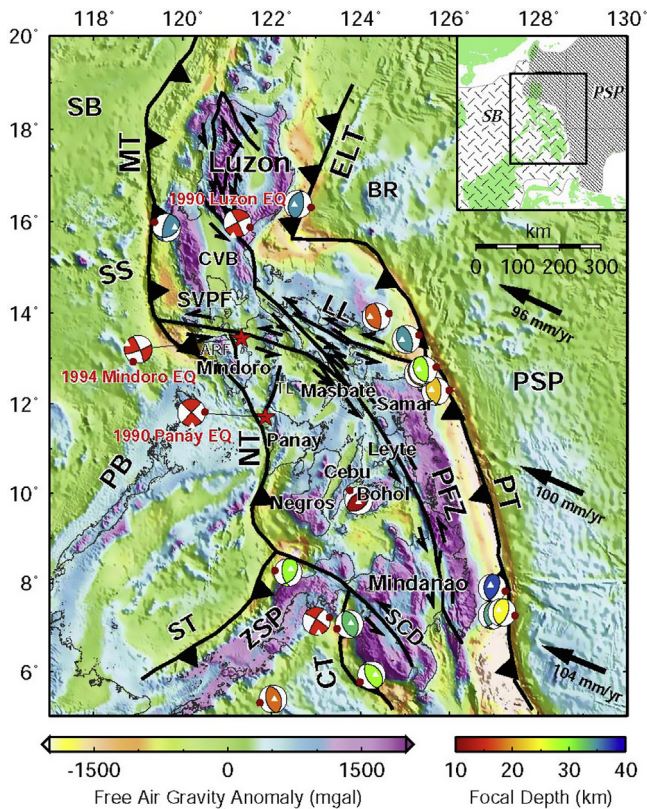
Fig. 1. Map showing the tectonic setting of the Philippine region. Free-air gravity anomalies are superimposed on the bathymetry of the study area. The bathymetry is from Sandwell and Smith (1997), and the gravity data are from Sandwell et al. (2014). The black arrows indicate the theoretical plate motion between the Sunda Block and the Philippine Sea Plate based on the NNR-MORVEL56 model (Argus et al., 2011). The epicenters and focal mechanisms of the large (Mw ≥ 7.0) earthquakes with focal depths ≤40 km are marked by the beach balls. The equal-area projections of the lower hemispheres of the focal spheres are plotted to show the orientation of the nodal planes, and the shaded areas are quadrants with compressional P-wave first motions. Circles and triangles on the focal spheres are P- and T-axes. The black lines are the main tectonic features modified from Yumul et al. (2009a, 2009b). T: Tablas; R: Romblon; S: Sibuyan; CVB: Central Valley Basin; PFZ: Philippine Fault Zone; LL: Legaspi Lineament; SCDL: Sindangan–Cotabato–Daguma Lineament; SVPF: Verde Passage Fault–Sibuyan Sea Fault; CT: Cotabota Trench; NT: Negros Trench; MT: Manila Trench; PT: Philippine Trench; ST: Sulu Trench; ELT: East Luzon Trough; BR: Benham Rise; PB: Palawan Block; SS: Scarborough Seamount; ZSP: Zamboanga-Sulu Peninsula; ARF: Aglubang River Fault; tl: Tablas Lineament. The upper-right figure shows the position of the study area at a smaller scale. EU: Eurasia Plate; PSP: Philippines Sea Plate; SB: Sunda Block.

2015). This indicates that this region is accumulating a large amount of elastic strain that can produce such large earthquakes.

Between the two subduction zones, the seismogenic region that has a large amount of seismic activity is defined as the Philippine Mobile Belt (PMB) (Gervasio, 1967), which consists of continental fragments, ophiolites and magmatic arc terranes (Ringenbach et al., 1993). Within the PMB, several active faults have developed in the Philippine Fault Zone (PFZ) in response to the compressional and shear stresses induced by the convergence between the PSP and Eurasian Plates. The PFZ crosscuts the PMB in an approximately NNW–SSE direction with a left-lateral strike-slip motion (Barrier et al., 1991; Aurelio et al., 1997) and accommodates the trench-parallel motion from the oblique convergence (Fitch, 1972; McCaffrey, 1992; Aurelio, 2000). The longest seismically active fault within the PFZ is the Philippine Fault, which is among the great continental strike-slip faults of the world (Bautista et al., 2001). There are two large fault branches of the PFZ, the Legaspi

Lineament (LL) and the Sibuyan Verde Passage Fault (SVPF), which intersect the Philippine Fault from the east and west, respectively, and to act as transfer faults (Fig. 1) (Beavan et al., 2001; Bischke et al., 1990; Yumul et al., 2008). The SVPF spreads out of the PFZ near Masbate and extends westward near the Manila Trench, whereas the LL connects the PFZ and the PT. However, previous studies also have demonstrated that the Philippine Fault, LL, and SVPF are three independent strike-slip faults based on the seismic reflection data (Aurelio et al., 1997). Additionally, in Mindanao the NW trending Sindangan-Cotabato-Daguma (SCD) Lineament is another left-lateral fault to accommodate elastic stress that is not consumed by the surrounding trenches in Mindanao (Yumul et al., 2009a, 2009b).

In addition to the active faults in the PMB, several oceanic bathymetric highs are located along the western boundary of the PMB: from north to south, the Scarborough Seamount (SS), the Palawan Block (PB) and the Zamboanga-Sulu Peninsula (ZSP) (Karig, 1975; Barrier et al., 1991; Pubellier et al., 2000; Bautista et al., 2001; Yumul et al., 2008) (Fig. 1). The continental, arc and ophiolite affinities generated in the central Mindanao area imply the presence of the collision between the ZSP and the PMB (Querubin and Yumul, 2001; Sherlock et al., 2003). Further north, the collision between the PB and the PMB is apparent and has resulted in several indentations related structures including micro-block rotations and ophiolite emplacements. (McCabe et al., 1985; Jumawan et al., 1998; Ramos et al., 2005; Yumul et al., 2005; Yumul, 2007). Based on a stratigraphic analysis, Karig (1983) proposed that the Southwest Mindoro Thrust Belt probably represents a section of the collision boundary between PB and PMB. Furthermore, the presence of a metamorphic suite and ophiolite complex observed in the Romblon Island group, which comprises Tablas, Romblon and Sibuyan (islands), and Panay Island is also believed to be a consequence of the PB–PMB collision (Dimalanta and Yumul, 2006; Yumul et al., 2009a, 2009b). In contrast to the western boundary of the PMB, only one oceanic bathymetric high, the Benham Rise (BR), has been observed on the eastern boundary of the PMB, which rams North Luzon on its eastern coast. The significant correlation between the shapes of the BR and the eastern border of North Luzon provides evidence to demonstrate that the effects of the collision may reach this region (Sajona et al., 1997; Lallemand et al., 1998; Bautista et al., 2001).

As described above, the Philippines is tectonically and seismically active, which is pervaded by large earthquakes. Therefore, it is important to assess the seismic potential for the entire Philippine region. To provide insights into the seismogenic characteristics and the regional deformation, it is critical to understand the state of stress in the crust (Hardebeck and Hauksson, 1999, 2001; Hardebeck and Michael, 2004, 2006). Previously, several studies have characterized the crustal deformation for the entirety of the Philippines or some part of the them using geodetic observations and earthquake focal mechanisms (Bautista et al., 2001; Galgana et al., 2007; Lin and Lo, 2013), particularly Hsu et al. (2012), who inverted stress tensors and proposed that the effective normal stress on the Philippine Fault in central Luzon would be low due to high fluid pressure. Note that only a few regions with stress tensors near the Philippine Fault were studied in Hsu et al. (2012). In this study, we attempt to reveal the spatial variations in the stress state for the whole Philippine region because it would be helpful for seismic hazard assessment, in particular, we are interested in whether the stress field is as spatially complex as the fault systems or whether the stress field is relatively homogeneous. A detailed description of the spatial variations of the stress field of the Philippines will provide critical constraints on crustal deformation and the geodynamic context for seismic hazard assessments.

2. Earthquake data and the stress inversion method

To determine the crustal stress field in the Philippine region, we used the final solutions of the GCMT catalog. On the basis of a surface wave analysis, the crustal thickness in the Philippine region has been estimated to be approximately 20–30 km (Tang and Zheng, 2013). In addition, the geodetic study has suggested that the average fault-locking depth is about 25 km, which implies that the crustal thickness is close to 25 km. (Galgana et al., 2007). Therefore, we selected events shallower than 40 km from the GCMT catalog by taking 30 km as the average crustal thickness and 10 km as the uncertainties in the crustal thickness and centroid depths of the potential events. In total, 1018 events were selected for further analysis (Fig. 2a). The average focal depth for most of the area is between 15 and 25 km (Fig. 2c).

We applied the damped stress inversion method from Hardebeck and Michael (2006), who introduced a damping parameter to smooth the difference between the stress tensors at two neighboring grid nodes to determine the stress fields. One of the merits of the damped stress inversion method is the avoidance of a subjective division of the earthquake focal mechanisms. Hence, the studied area was divided using a 1.0° by 1.0° grid, and each focal mechanism solution was assigned to the nearest grid node (Fig. 2a). The number of events for each grid node is shown in Fig. 2b, and grid nodes with at least eight events were used for the stress tensor inversion.

For the damped stress inversion, we first performed an inversion for a series of damping parameters to obtain the L-curve that represents the trade-off between the model length and the data variance, and then visually selected a value of 1.0 at the corner of the trade-off curve as the optimal damping value (Fig. 3).

3. Results

From the stress tensor inversion, we obtain the azimuths and plunges of the three principal stresses axes σ_1, σ_2 and σ_3 ($\sigma_1 \geq \sigma_2 \geq \sigma_3$), the stress ratio ($\Phi = (\sigma_2 - \sigma_3)/(\sigma_1 - \sigma_3)$) and the corresponding 95% confidence level from 1000 bootstrap re-samples for each grid node. The maximum principal stresses axis (σ_1) is conventionally defined as the compressional stress axis, and the minimum principal stress axis (σ_3) is the extensional stress axis (Angelier, 1979). To facilitate our discussion, the azimuth and plunge of the compressional (σ_1) and extensional (σ_3) stress axes are displayed in a lower hemisphere projection,
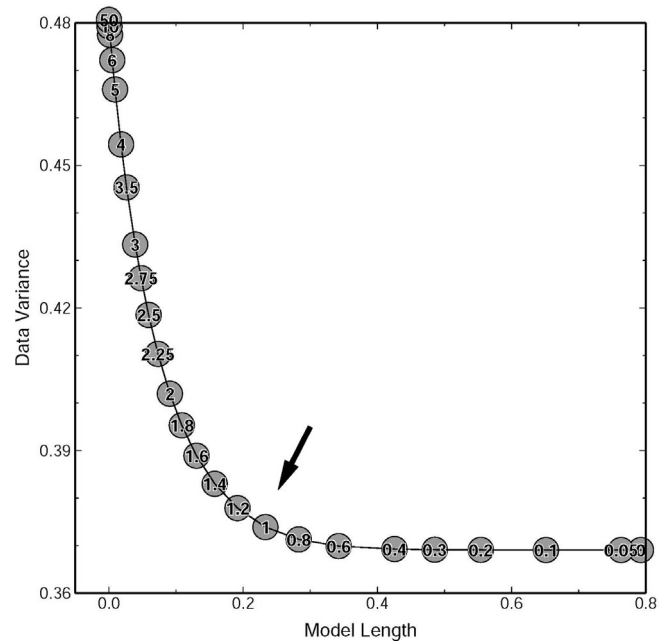

Fig. 3. Trade-off curve showing the relation between the model length and data variance for different choices of the damping parameters (circles). The model length is represented by the L2 norm (or Euclidean length) of the vector containing the differences between each stress tensor component for each pair of adjacent grid points; the data variance is the misfit between the data and the predictions of model (Hardebeck and Michael, 2006). The arrow indicates the optimal damping value.

in which the background color represents the stress ratio (Fig. 4a). The azimuthal uncertainties of σ_1 and σ_3 are also shown in Fig. 4b and c, respectively. The stress ratios in a few grid nodes with large azimuthal uncertainties are approximately 1 and 0 (Fig. 4), which could be explained by the stress permutation (Hu and Angelier, 2004).

Hardebeck and Hauksson (2001) showed that stress orientations can be well-resolved only if diverse focal mechanisms are available, one measure of which is the root-mean-square angular difference from the mean focal mechanism, which should be larger than 40 degrees when using focal mechanisms with nodal plane ambiguities between 10 and 20 degrees. Previous studies have demonstrated that the average uncertainty in the principal axes
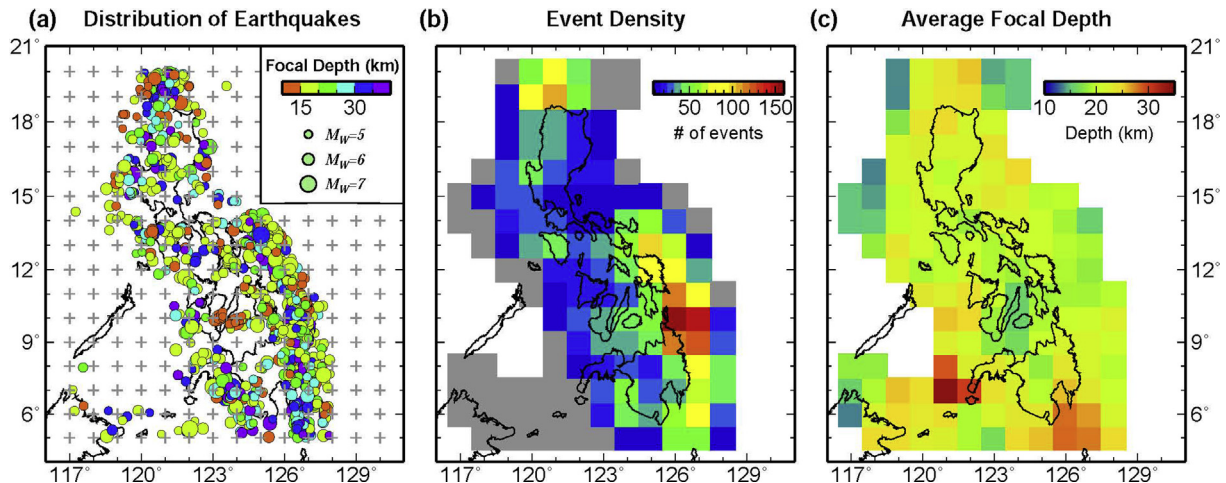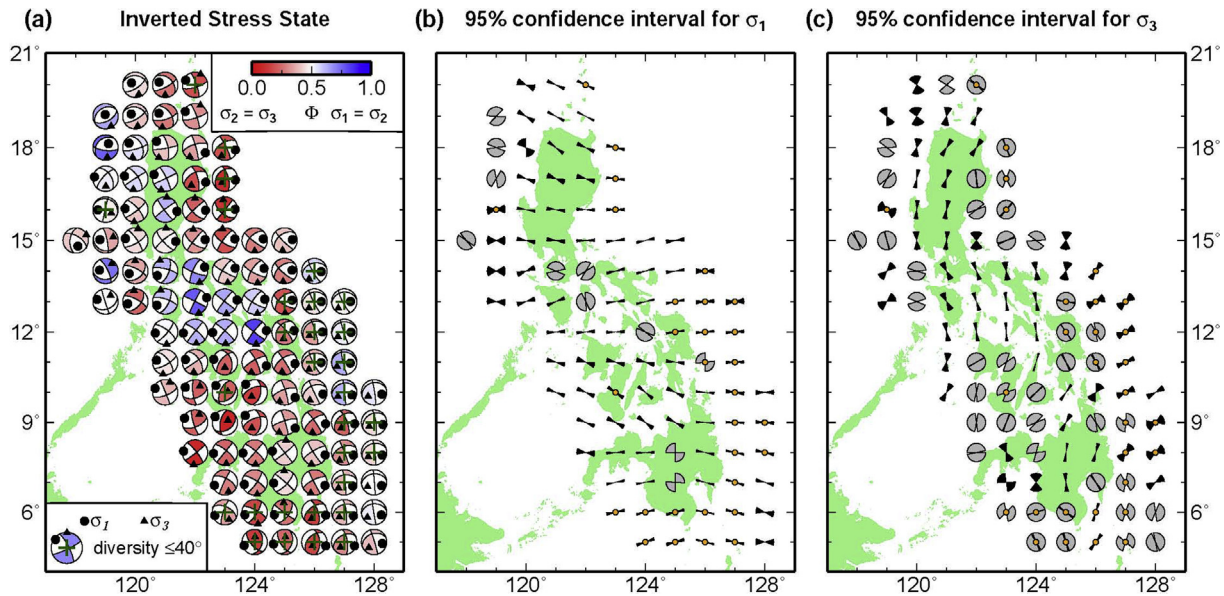

Fig. 2. (a) Distribution of the grid nodes (crosses) with a grid interval of 1.0° and the epicenters and magnitudes of the earthquakes from the GCMT catalog (circles) used for the analyses. (b) Number of events for each node. The grid nodes shaded in gray had too few (<8) events to be used in the stress inversion. (c) Average focal depths of the events utilized for each node.

Fig. 4. Results of the inverted crustal stress field in the area of the Philippines (a) for each grid node, the orientations of σ_1 and σ_3 are marked by the equal-area projections of the lower hemispheres of the focal spheres, and the colors show the corresponding ratios of the stress differences, $\Phi = (\sigma_2 - \sigma_3)/(\sigma_1 - \sigma_3)$. A node is marked by a green cross if the diversity of the focal mechanism dataset is $\leq 40°$, which indicates that the dataset may not be able to sufficiently constrain the orientation of the inverted principle stress axes. In (b) and (c), the 95% confidence intervals at each grid node for the σ_1 and σ_3 directions were estimated from 1000 bootstrap re-samplings, and the nodes are marked by red circles if the diversity of the focal mechanism dataset is $\leq 40°$. (For interpretation of the references to colour in this figure legend, the reader is referred to the web version of this article.)

of GCMT earthquake focal mechanisms is ∼15 degrees (Helffrich, 1997; Frohlich and Davis, 1999;Frohlich, 2001). Therefore, we labeled the grid nodes with crosses and circles to indicate whether the focal mechanism diversity is less than 40 degrees in Fig. 4a–c, respectively. On the other hand, grid nodes with focal mechanism diversities greater than 85 degrees may indicate that the stress field is not uniform and may violate the basic assumption of the stress inversion (Gephart and Forsyth, 1984; Michael, 1984; Y.-M. Wu et al., 2010). It can be observed from that none of the grid nodes have focal mechanism diversities larger than 85 degrees (Fig. 4a), which indicates that the stress regime at each grid node is rather homogeneous in our study area. To reveal the variation in the direction of σ_1 with respective to the relative plate motion direction, we compute the difference between the direction of σ_1 and the average direction of the theoretical plate motion (294°N) in the Philippines (Argus et al., 2011) (Fig. 5a). Simultaneously, we estimate the average differences of the stress azimuth at each grid node with its immediate neighboring nodes for σ_1 and σ_3 to quantitatively illustrate spatial variations in stress directions (W.-N. Wu et al., 2010) (Fig. 5b and c).

3.1. Spatial variations of compressional stress axis (σ_1)

In general, σ_1 trends along the E-W direction for most of the area over the entire Philippines and is sub-perpendicular to the strike of the main trench systems (Fig. 5a and b). For most of the σ_1-axes, the stress orientation varies between −30 and 10 degrees from the average relative plate motion direction (294°N). Under the predominantly E-W stress regime, slight to significant variations can still be observed in some areas (Fig. 5a): (1) Along the eastern subduction system of the PMB, which includes the PT and ELT, σ_1 is generally consistent with the regional stress. Only a minor counterclockwise rotation of σ_1 occurs along the PT; it is in the NWW-SEE direction in the south and the NEE-SWW direction in the north. (2) In contrast, there are greater variations in the stress direction and the plunge in the western subduction zones. The direction of σ_1 for the southernmost trench system,

the Cotabato Trench, intersects the plate motion at greater than 30° (Fig. 5a), which corresponds perfectly to the trench-normal orientation. Along the Negros Trench, the strike of the trench changes so rapidly that makes it difficult to determine the relation between the direction of σ_1 and the trench orientation. However, the direction of σ_1 seems to be consistent with that in the surrounding area. The northernmost subduction system, the Manila Trench, is the only system where we observed significant variations in stress along a single trench. σ_1 trends normal to the trench in the area located near the SB (∼17.5°N) and south of the SB, but it becomes unstable and shows inhomogeneous directions to the north of the SB. (3) There are distinct changes in σ_1 relative to the regional stress between the two opposite subduction zones in the central-western portion of the Philippines (∼8.5°N–14.5°N), including the Mindoro, Panay, Negros, Cebu and Bohol Islands (Fig. 5b). The stress signature of the area comprises a systematic counterclockwise rotation of σ_1 from south to north. Centered at the PB, the σ_1-axes change their direction from NE–SW in the north, which is approximately less than −30 degrees from the direction of the relative plate motion, to NW–SE in the south, which is approximately larger than 10 degrees from the direction of the relative plate motion (Fig. 5a). (4) Another area where the direction of σ_1 varies largely from the regional stress regime is located in the Luzon region. σ_1 across the entire area of the northern part of Luzon Island (between 16.5°N and 19°N) is characterized by a NW-SE trending direction, which is approximately consistent with the direction of the relative plate motion or has a slight directional difference of less than 20 degrees (Fig. 5a). This stress regime does not extend to the southern part of Luzon Island, where the predominant E-W trending regional stress persists.

3.2. Spatial variation of extensional stress axis (σ_3)

As shown in Fig. 5c, the regional σ_3 trends primarily along the N-S direction and has systematic variations from south to north. Starting from the N-S direction in the most southern area of the PMB (∼6°N), σ_3 alters to the NNE-SSW direction at the latitude
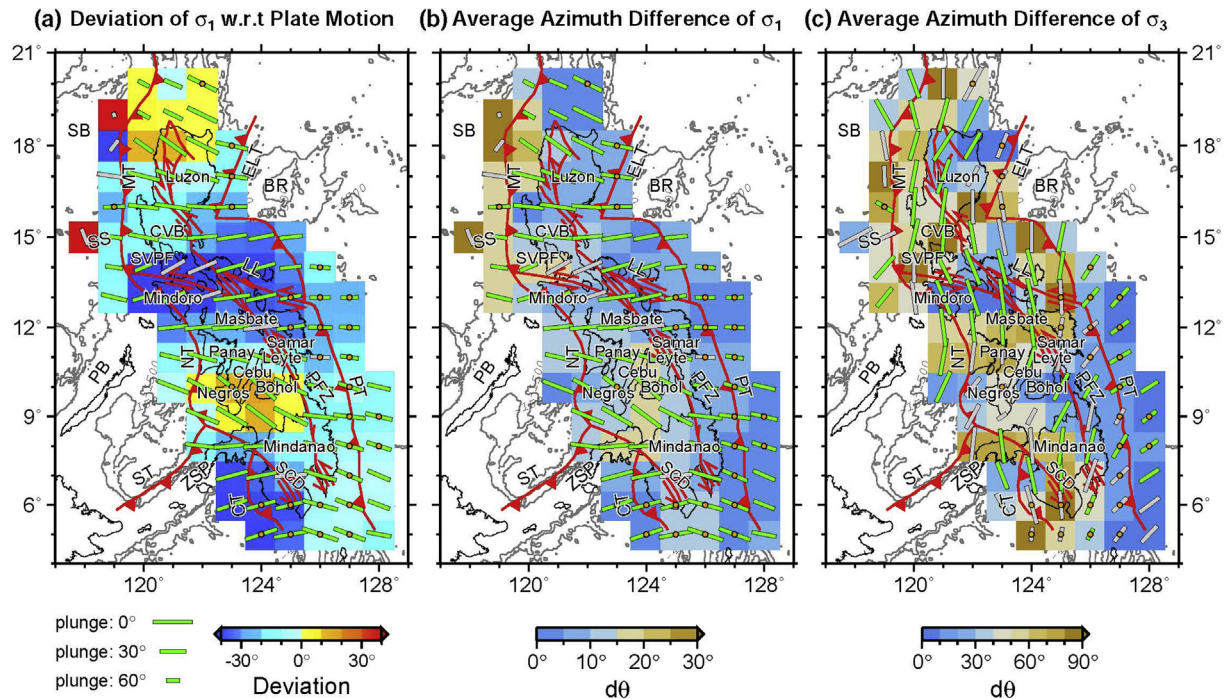
Fig. 5. (a) The azimuthal differences between the σ_1 direction and the average relative plate motion (N294°) at each node are scaled using colors. The positive and negative values indicate that σ_1 rotates clockwise and counterclockwise with respect to the relative plate motion direction, respectively. (b) The orientation of σ_1 at each grid node is marked by a green or a gray bar whose length is proportional to the plunge angle. The diversity of the focal mechanism dataset is $\leq 40°$ at the grid nodes marked by gray bars. The color beneath each node is the average difference in the σ_1 direction with respect to the neighboring nodes. (c) Similar to (b) but for σ_3. Bo: Bohol Island; Ce: Cebu Island; Ma: Masbate Island; Ne: Negros Island; Pa: Panay Island; Sa; Samar Island. (For interpretation of the references to colour in this figure legend, the reader is referred to the web version of this article.)

where the ZSP enters the PMB ($\sim$8.5°N). It then pivots counterclockwise toward the north and has a NNW-SSE direction when it reaches 14.5°N. Moving north, σ_3 suddenly rotates clockwise and attains a NNE-SSW direction at18°N. Although the change in σ_3 appears to be gentle, but in some local areas are remarkably different from the regional stress configuration. Among those areas, (1) The entire PT is characterized by a NE-SW σ_3 direction rather than a N-S direction. If we compare the average differences of the stress azimuth at each grid node with its immediate neighboring nodes, we find that σ_3 along the PT is extremely homogeneous, similar to the pattern in the distribution of σ_1 (Fig. 5b). (2) Following the σ_1 distribution, the direction of σ_3 has large variations along the western subduction zones. The Cotabato Trench and the Negros Trench are characterized by a trench-parallel σ_3. In contrast, the configurations of σ_3 in the Manila Trench is rather complicated, that is, the direction of σ_3 corresponds well to the regional N-S direction in the northern part, but abruptly changes to NE-SW when it goes south of 15.5°N, where the SS appears on the oceanic plate. (3) The most complicated pattern in the distribution of σ_3 is in the central-western portion of the area of the Philippines around the Negros, Cebu and Bohol Islands, where the orientation of σ_3 is different from its neighboring areas and the plunge has steep angle. (4) Finally, the direction of σ_3 in northern Luzon (north of 16.5°N) rotates clockwise from a NW-SE direction in the west to a NE-SW direction in the east. The transition of the N-S direction in the south to the more radial NW-SE and NE-SW direction in the north shows a fan-shaped stress rotation, which is particularly significant in the marine area.

4. Discussion

The average maximum stress distribution conforms to the regional tectonic configuration, which is the strong convergence

setting of the Sunda and the Philippine Sea plates. Previous global studies have well demonstrated that the direction of σ_1 is generally parallel/sub-parallel to the absolute or relative plate motions (e.g., Heidbach et al., 2007). However, the E-W trending dominant σ_1 indicates that the convergence direction is approximately 30 degrees from the direction of the relative plate motion, which is 294°. This observation suggests that the N-S trending subduction systems along the two sides of the PMB should play important roles on the stress adjustment, which accommodates the trench normal convergent motion from the oblique convergence and affects the stress distribution of the area in the vicinity of the trench. However, smooth variations in σ_1 could still occur when the trench direction or the degree of stress partitioning change, as demonstrated by the counterclockwise rotation of σ_1 along the PT from south to north. On the other hand, the PMB area is under E-W compression, an N-S trending extensional stress should be therefore expected, which overall is in good agreement with our result.

4.1. Identification of different stress regimes

On the basis of the spatial variations in σ_1 and σ_3, we determined the regional dominant stress configuration of the area of the Philippines. Different stress variations can also be distinguished simultaneously in some local tectonic environments. Herein, we have divided the entire PMB into four sub-areas that have significantly different properties.

(1) The region along the western subduction system, the PT and the East Luzon Trough:

In this region, in terms of the average difference of stress azimuth for each grid node with its immediate neighboring nodes,

the directions of σ_1 are rather homogeneous (Fig. 5b and c) and approximately sub-perpendicular to the strike of the trench. This observation suggests that the stress field along the eastern portion of the PMB should be largely influenced by the subduction process of the PSP beneath the PMB and only bears minor effects from the local tectonic structures. On the contrary, σ_3 have different patterns, with a trench-parallel direction for the ELT and a trench-perpendicular direction along some parts of the PT. The trench-perpendicular σ_3 in the crustal portion of the subduction system is generally considered to be a response to the bending of the subducted plate (Kao and Chen, 1991; Kao et al., 1998; Wu et al., 2009). In addition, the intermediate plunge angle of σ_1 in the PT area could reflect the down-dip movement of the subducted plate. Thus, both the compressive and extensional stress distributions confirm the subduction dominated stress regime along the PT. However, the scarcity of earthquakes and the low diversity in the focal mechanism pattern along the ELT could generate large uncertainty in the stress inversion for σ_3. Therefore, the origin for the trench-parallel extension effect along the ELT is not discussed here.

(2) The Manila subduction system

The Manila Trench belongs to the western subduction systems in the Philippines, which generally shows a stress regime similar to the eastern one. However, the Manila Trench possesses a unique stress signature with an obvious variation along the trench. In its southern portion (between ~13°N and 15°N), the σ_1 configuration is also similar to that along the PT, which is a nearly trench-perpendicular stress direction with intermediate plunge. This stress configuration may reflect the flexural bending of the Sunda Block beneath the PMB. However, a dramatic change in σ_3 direction appears to the north of 15°N, and the stress direction varies rapidly with respect to its immediate neighboring nodes (light brown color at 15°N in Fig. 5c). In particular, the direction of σ_3 is in good agreement with the regional N-S direction in the northern part, whereas it changes to NE-SW abruptly when it goes to the south of 15°N. This sudden transition in σ_3 seems to correspond to the position where the SS enters the PMB, although there is large azimuthal uncertainty in the direction of σ_3. Coincidently, the bathymetric highs and gravity anomalies on the two sides of 15°N are also characterized by different signatures: visible trench depression and relatively low gravity anomalies in the southern portion; while unobvious trench morphology and insignificant gravity anomalies in the northern part (Fig. 1). Thus, the distinct signature of the stress and geological evidence on the two sides of 15°N may suggest the possible influence of the SS subduction on the subduction process. Note that the change in σ_3 appears to be limited to the oceanic portion and the fore-arc area, but the direction of σ_1 does not have a corresponding change. Further studies are needed to determine the origin of this discrimination. The interaction between the SS and the PMB is poorly documented in the literature, and the potential influence of the subduction of the seamounts remains unknown. The stress variation observed in our study may provide critical constraints for further investigations. For example, the seamount subduction may be one of the origins for the dissimilar stress pattern observed along the Philippine and Manila Trenches, which may create different seismogenic characteristics of the two subduction systems.

(3) Area under the collision of the PB and the PMB:

As described previously, the central-western part of the area of the Philippines (between 8.5°N and 14.5°N) is characterized by a fan-shaped stress pattern with mostly very shallow plunges for both σ_1 and σ_3. With respect to the σ_1 direction, at 12°N

where the PB enters the PMB, σ_1 for its northern grid nodes (e.g., Mindoro) rotates counterclockwise, whereas in the other islands located to the south, such as Panay, Negros, Leyte and Bohol, σ_1 pivots clockwise. Such a stress pattern is consistent with the interpretation of micro-block rotation induced by the collision of the PB and the PMB on the basis of a variety of observations from paleo-magnetic (McCabe et al., 1982; Yumul et al., 2003), and geological studies (McCabe et al., 1985; Jumawan et al., 1998; Ramos et al., 2005; Yumul et al., 2005; Yumul, 2007).

Based on the stress distribution illustrated in Fig. 5a, the northern boundary of the fan-shaped stress pattern, which is E-W trending σ_1 in the west and systematically clockwise rotation toward the east, appears to be located between the CVB and SVPF (~14.5°N), whereas the southern boundary coincides with the area where the SS enters the PMB (~8.5°N). The σ_1 direction in some portions with the fan-shaped feature (between 11.5°N and 14.5°N) is similar to the regional dominant E-W region stress regime and cannot be distinguished easily from σ_1 in the neighboring tectonic system on the eastern side. According to the shear partitioning model (e.g., Fitch, 1972), the oblique convergence between the PSP and SB bounding the Philippine Archipelago mostly is taken up by the left-lateral PFZ (Fitch, 1972; Barrier et al., 1991; Aurelio, 2000;). However, a visible change in σ_1 on the two sides of the PFZ appears in its southern portion (between 7.5 and 11.5°N). σ_1 trends NW-SE to the west of the PFZ, whereas it changes to WNW-ESE to the east of the PFZ. This boundary is even more significant when we calculate the average difference of the stress azimuth within each grid node with its immediate neighboring nodes (Fig. 5b). The large difference in the stress azimuth observed on the two sides of the PFZ indicates that the PFZ is the best candidate for the eastern boundary of the fan-shaped stress pattern. In conclusion, we have determined that the northern part of the SVPF, the PFZ and the Mindanao are the northern, eastern and southern boundaries affected by the PB-PMB collisional process, respectively. It is worth noting that the ZSP enters the PMB at the southern boundary, and, surprisingly, the collision between the ZSP and the PMB has not left any significant trace on the stress configuration. The phenomenon could be caused by the relatively stronger magnitude of the collision between the PB and PMB, which covers the effect of the ZSP-PMB collision. Otherwise, we suggest that the ZSP-PMB collision may have already ceased, or the ZSP has not collided with the PMB in Mindanao, which could also explain why no related responses can be observed in the present-day stress regime. Unfortunately our inversion result cannot confidently resolve these arguments.

Regarding the location and stress distribution, the stress regime along the Negros Trench (from 9°N to 11°N) seems to be in agreement with that in the fan-shaped areas generated by the PB-PMB collision. This stress pattern infers that the PB-PMB collision should have a large influence on the stress regime of the Negros subduction system that might modify its original subduction-related characteristics. However, further investigation is needed to confirm this assumption.

In the collisional area, given that the direction of σ_1 is an indicator for the plate convergent direction, the direction of σ_3 is reasonably the proxy to sense the extensional direction and the related movement of the extruded crustal material induced by the compressive force during the collisional process. Thus, relatively higher escapement of material could be expected in the area where the collisional process is most active and may produce local extensional environments, even though the tectonic environment of the area is purely characterized by strike-slip type focal mechanisms (Yumul, 2007; Lin and Lo, 2013). With the decrease in the effects of the collision to the south and to the north of the PB, the degree of rotation should also be reduced, and the escape of

material would be difficult. Under this assumption, the sudden change in the σ_3 plunge at the southern portion of fan-shaped area could be successfully explained by the increasing horizontal stress caused by the accumulation of excess material coming from the active collision area.

(4) The northern Luzon Island area:

Similar to the central-western Philippines, the stress distribution in the northern Luzon Island area also indicates a symmetrical rotation. However, a relatively smaller rotation in σ_3 regarding to that in the central-western Philippines is observed. σ_1 in northern Luzon is almost parallel to the direction of the relative plate convergent motion and has slight variations of approximately 10 degrees (Fig. 5a). This σ_1 configuration indicates that the continuously northwestward advance of the PSP is probably responsible for the stress source in this region, which could be related to the left-lateral movement along the PFZ. Then, the excess material brought by the left-lateral movement could spread to the unbounded direction and form an extensional fan-shaped environment as shown by the σ_3 distribution in this area. Ringenbach et al. (1993) suggested that under the pinching effect of the BR and the PB, the eastern PMB could extend northward along the PFZ. Lin and Lo (2013) further proposed that the necking effect between the BR and the PB associated with the PMB collision may induce the lateral extrusion of the northeastern Luzon block, which is evidenced by earthquake-induced gravitational energy change. Meanwhile, the southern boundary of the rotated σ_3 fan-shaped feature appears to lie between 14°N and 15°N, where the compressive effect due to the collision process between the PB and the PMB seems to cease (Fig. 5a and b). Thus, instead of a combined pinching effect by both the BR and the PB, we suggest that the northward movement of the northern Luzon area may simply be due to the excessive left-lateral motion along the branch of the PFZ.

4.2. Stress transition boundary

From the preceding description, σ_3 and part of the σ_1 distribution show distinct patterns on the two sides of the PFZ: a southward clockwise rotation in the directions of σ_1 and σ_3 on its western side from 9°N to 11°N. In particular, the σ_1-axes are oriented NW-SE on the eastern side of the PFZ but have NWW-SEE direction from 9°N to 11°N. Such a significant variation is the direction of σ_1 across the PFZ suggesting that the PFZ is a stress boundary to distinguish the stress states in the PT subduction from the PB-PMB collision. In addition, the northern boundary of the PB-PMB collision zone coincides with a branch of the PFZ, northern part of the SVPF. Bounded by the PFZ, the stress state in the northern Luzon Island area is significantly different from that in its southern part. As a consequence, the PFZ seems to not only accommodate the partitioned left-lateral motions from the oblique convergence but also to be a boundary condition to separate stress regimes in different tectonic units. In our results, we also observed that the southern boundary of the PB-PMB collision coincides with the position of ZSP. Furthermore, the stress patterns on each side of the SS visibly vary along the Manila Trench, indicating that the presence of the oceanic bathymetry highs can produce certain effects on the stress environment, as already evidenced by several earlier studies (Wu et al., 2009; W.-N. Wu et al., 2010). Consequently, the stress distribution in the area of the Philippines demonstrates again that stress transitions can occur not only by large tectonic structures, such as the trenches and fault systems but also in the vicinity of subducted or collided seamounts, which can large effect on the configuration of the regional stress.

4.3. Stress field complexity and rupture plane ambiguity

In Fig. 4a, the inverted stress regime presented by the equal-area projection of the lower hemisphere is characterized by strike-slip faulting along most faults within the PMB, which is in good agreement with the field observation. However, the inverted stress field along the PT seems to be inconsistent with the theoretical expectation that the σ_3 is vertical and the σ_1 is horizontal for a typical thrust fault with the plunge of 30° (Fig. 6a). That is, our inverted stress regime appears the strike-slip faulting domination along the PT rather than the thrust faulting type. Even though the inverted σ_1 orientations do not coincide with the P-axes of the large earthquakes, both of them generally still lie in the same compressional quadrant of the focal sphere. Moreover, visible difference can be observed between the T-axis and the inverted σ_3, e.g. the large earthquakes occurred along the PT showed near vertical T-axes, whereas the inverted σ_3 were characterized by the plunge of 30–60° (Fig. 6a). It is worthy mention again that the stress inversion along the subduction zones was performed by combining the events occurred in the overriding plate, subduction interface and intra-slab. In other words, our dataset samples not only earthquakes located directly on the subduction interface but also in a region around the plate interface to constrain the stress field acting on the plate interface. Consequently, the inverted stress field along the subduction zone may not completely present the stress state of the plate interface (thrust-faulting type). Besides, along the subduction zone, the stress field may be dominated by the plate bending or back-arc spreading or rifting, and thus the extensional stress axis σ_3 may not be vertical. The latest global study of the stress field in the subduction zones also demonstrated that the stresses in some subduction zones are not Andersonian (Hardebeck, 2015) and σ_3 may not be necessarily vertical for some situations, which is consistent with our results.

In addition, two large strike-slip earthquakes, the 1990 M_s 7.8 Luzon earthquake and the 1990 M_w7.1 Panay earthquake, occurred within the PMB, which P- and T-axes are in consistency with our inverted stress regime (Fig. 6b). The rupture plane of the 1990 Luzon earthquake could be dominated by the strike of PF, which demonstrates a left-lateral movement. However, the rupture plane of the 1990 Panay earthquake was suggested to be associated with the Tablas Lineament, a dextral NE-SW striking structure, not related with the NT. For the other large strike-slip earthquake, the 1994 M_w7.1 Mindoro earthquake, its P- and T axes are significantly different from our inverted stress directions. Nevertheless, the P-axis and the inverted σ_1 are still located at the same quadrant of the focal sphere, which suggests that the stress state should still be consistent. It shall be noted that even though the 1994 Mindoro earthquake occurred near the SVPF, previous studies showed that its rupture plane was related to the N-S trending Aglubang River Fault with a dextral motion rather than along the SVPF with a sinistral movement (Simplina-Manahan, 2004). The result concluded from the observation for the strike-slip events shows that the rupture plane of an earthquake may be dominated by local structures (e.g., active faults). The inverted stress regime can only provide the stress orientations and cannot determine the location and the true rupture plane of an earthquake, which could be an inevitable limit of our method. However, this restriction may be resolved if the geological structures have been well defined in the area. Finally, the calculation grid used for our stress inversion is as large as one degree by one degree (about 100 km by 100 km) restricted by the number of available earthquakes. This grid spacing may be too large to illustrate the influence caused by the local effects and limits the resolution and precision of our result, which could be improved by collecting more earthquakes through the deployment of local seismic networks.
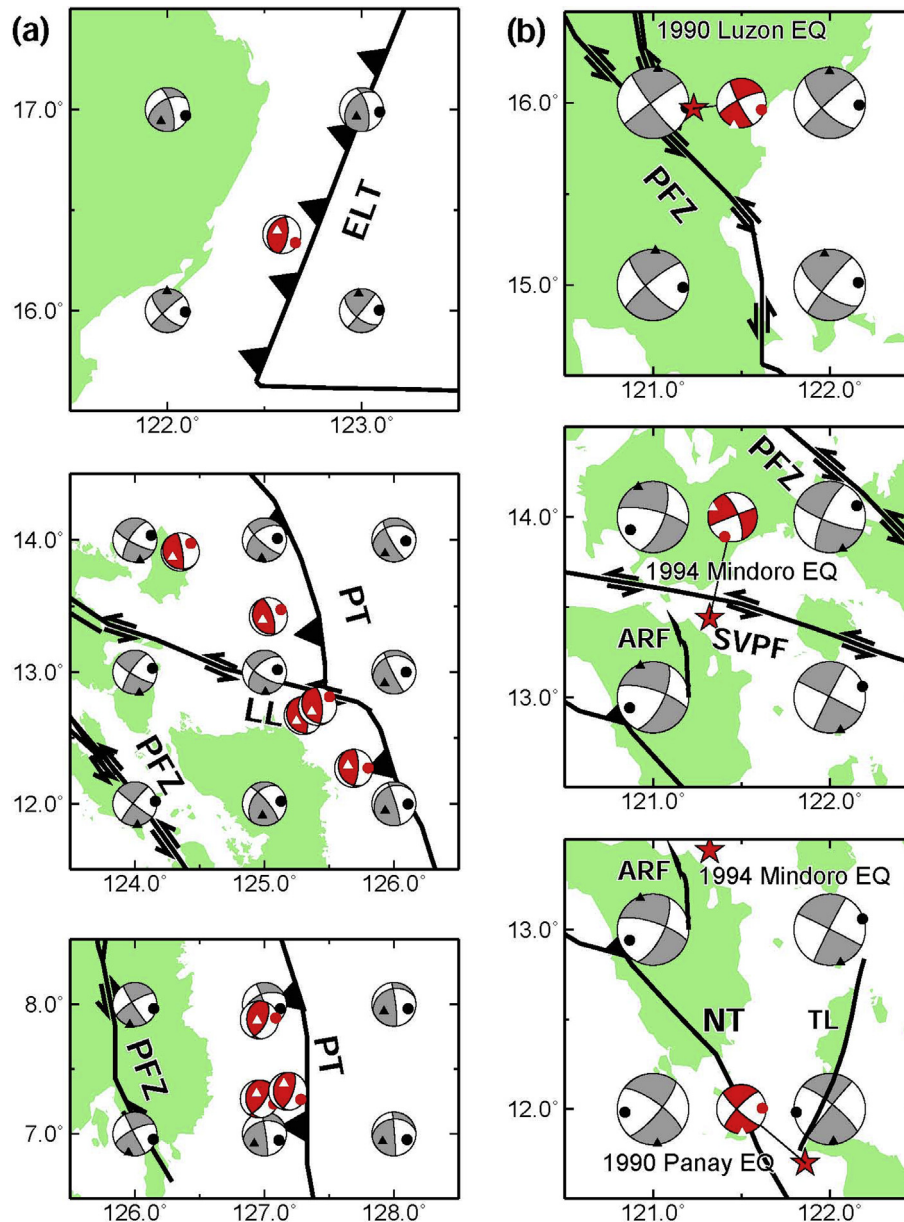
Fig. 6. The relationships between the focal mechanism of large ($M_w \geq 7$) earthquakes (shaded with red color) and the inverted stress regime (shaded with gray color). Red circles and withe triangles are P and T axes of large earthquakes, respectively; Black circles and triangles are σ_1 and σ_3 of inverted stress field, respectively. (a) Focus on discussion on the inconsistency between the earthquake focal mechanisms and the inverted stress regimes along the PT. (b) Focus on discussion on the relationships among the three large strike-slip earthquakes, local structures and inverted stress regimes. (For interpretation of the references to colour in this figure legend, the reader is referred to the web version of this article.)

5. Conclusions

In this study, we applied an improved stress inversion method using the focal mechanism solutions to comprehensively reveal the stress field in the area of the Philippines, which enabled us to determine the spatial variations in the stress regime and to analyze the roles of the main geological structures. Our results show that the entire area of the Philippines is generally sustaining a strong convergence between the Sunda and Philippine Sea Plate, including subduction and collision processes. The direction of σ_1 trends generally in the E-W direction, which suggests that the trench-normal component from the oblique convergence could be the primary source of the stress regime. The effect induced by the PB-PMB collision process dominates a fan-shaped stress pattern that occupies most the western portion of the PMB. Separating the subduction-dominated stress regime in the east and the collisional regime in the southwest, the PFZ appears to be the main stress boundary of the PMB zone. Bounded by the northernmost branch of the PFZ, the northern and southern portions of Luzon Island possess different stress conditions. The stress distribution in the southern Luzon area is identical to the regional E-W trending stress configuration, whereas it appears to be related to the NW-SE relative plate motion in the northern Luzon area. In summary, the seismic activity and geological evaluations is closely correlated with the stress state in the corresponding areas. Based on this work, the main stress regimes in the area of the Philippines have been determined and could become the basis of future geo-hazard assessments and geodynamic investigations.

Acknowledgement

References

Angelier, J., 1979. Determination of the mean principal directions of stresses for a given fault population. Tectonophysics 56, 17–26.

Argus, D.F., Gordon, R.G., DeMets, C., 2011. Geologically current motion of 56 plates relative to the no-net-rotation reference frame. Geochem. Geophys. Geosyst. 12, Q11001. http://dx.doi.org/10.1029/2011GC003751.

Aurelio, M.A., 2000. Shear partitioning in the philippines: constraints from philippine fault and global positioning system data. Island Arc. 9, 584–597.

Aurelio, M., Barrier, E., Gaulon, R., Rangin, C., 1997. Deformation and stress states along the central segment of the Philippine Fault: implications to wrench fault tectonics. J. Asian Earth Sci. 15, 107–119.

Barrier, E., Huchon, P., Aurelio, M., 1991. Philippine fault: a key for Philippine kinematics. Geology 19, 32–35.

Bautista, B.C., Bautista, M.L.P., Oike, K., Wu, F.T., Punongbayan, R.S., 2001. A new insight on the geometry of subducting slabs in northern Luzon, Philippines. Tectonophysics 339, 279–310.

Beavan, J., Silcock, D., Hamburger, M., Ramos, E., Thibault, C., Feir, R., 2001. Geodetic constraints on postseismic deformation following the 1990 Ms 7.8 Luzon earthquake and implications for Luzon tectonics and Philippine Sea plate motion. Geochem. Geophys. Geosyst. 2 (9). http://dx.doi.org/10.1029/2000GC000100.

Bird, P., 2003. An updated digital model of plate boundaries. Geochem. Geophys. Geosyst. 4 (3). http://dx.doi.org/10.1029/2001GC000252.

Bischke, R.E., Suppe, J., del Pilar, R., 1990. Geodynamic evolution of the Eastern Eurasian Margin A new branch of the Philippine fault system as observed from aeromagnetic and seismic data. Tectonophysics 183, 243–264.

Dimalanta, C.B., Yumul, G.P., 2006. Magmatic and amagmatic contributions to crustal growth in the Philippine island arc system: comparison of the Cretaceous and post-Cretaceous periods. Geosci. J. 10, 321–329.

Dziewonski, A.M., Chou, T.-A., Woodhouse, J.H., 1981. Determination of earthquake source parameters from waveform data for studies of global and regional seismicity. Phys. Earth Planet. Int. 86, 2825–2852.

Fitch, T.J., 1972. Plate convergence, transcurrent faults, and internal deformation adjacent to Southeast Asia and the Western Pacific. J. Geophys. Res. 77, 4432–4460.

Frohlich, C., 2001. Display and quantitative assessment of distribution of earthquake focal mechanisms. Geophys. J. Int. 144, 300–308.

Frohlich, C., Davis, S.D., 1999. How well constrained are well-constrained T, B, and P axes in moment tensor catalogs? J. Geophys. Res. 104, 4901–4910.

Galgana, G., Hamburger, M., McCaffrey, R., Corpuz, E., Chen, Q., 2007. Analysis of crustal deformation in Luzon, Philippines using geodetic observations and earthquake focal mechanisms. Tectonophysics 432, 63–87.

Gephart, J.W., Forsyth, D.W., 1984. An improved method for determining the regional stress tensor using earthquake focal mechanism data: application to the San Fernando earthquake sequence. J. Geophys. Res. 89, 9305–9320.

Gervasio, F.C., 1967. Age and nature of orogenesis of the philippines. Tectonophysics 4, 379–402.

Hardebeck, J.L., 2015. Stress orientations in subduction zones and the strength of subduction megathrust faults. Science 349, 1213–1216.

Hardebeck, J.L., Hauksson, E., 1999. Role of fluids in faulting inferred from stress field signatures. Science 285, 236–239.

Hardebeck, J.L., Hauksson, E., 2001. Crustal stress field in southern California and its implications for fault mechanics. J. Geophys. Res. 106, 21859–21882.

Hardebeck, J.L., Michael, A.J., 2004. Stress orientations at intermediate angles to the San Andreas Fault, California. J. Geophys. Res. 109. http://dx.doi.org/10.1029/2004JB003239.

Hardebeck, J.L., Michael, A.J., 2006. Damped regional-scale stress inversions: methodology and examples for southern California and the Coalinga aftershock sequence. J. Geophys. Res. 111, B11310. http://dx.doi.org/10.1029/2005JB004144.

Heidbach, O., Reinecker, J., Tingay, M., Müller, B., Sperner, B., Fuchs, K., Wenzel, F., 2007. Plate boundary forces are not enough: second- and third-order stress patterns highlighted in the World Stress Map database. Tectonics 26 (6). http://dx.doi.org/10.1029/2007TC002133.

Helffrich, G.R., 1997. How good are routinely determined focal mechanisms? Empirical statistics based on a comparison of Harvard, USGS and ERI moment tensors. Geophys. J. Int. 131, 741–750.

Hsu, Y.-J., Yu, S.-B., Song, T.-R.A., Bacolcol, T., 2012. Plate coupling along the Manila subduction zone between Taiwan and northern Luzon. J. Asian Earth Sci. 51, 98–108.

Hu, J.-C., Angelier, J., 2004. Stress permutations: 3-D distinct element analysis accounts for a common phenomenon in brittle tectonics. J. Geophys. Res. 109, B09403. http://dx.doi.org/10.1029/2003JB002616.

Jumawan, F., Yumul, G., Tamayo, R., 1998. Using geochemistry as a tool in determining the tectonic setting and mineralization potential of an exposed upper mantle-crust sequence: example from the Amnay Ophiolitic complex in occidental Mindoro, Philippines. J. Geol. Soc. Philippines 53, 24–48.

Kao, H., Chen, W.-P., 1991. Earthquakes along the Ryukyu-Kyushu arc: strain segmentation, lateral compression, and the thermomechanical state of the plate interface. J. Geophys. Res. 96 (21), 21443–21485.

Kao, H., Shen, S.-S.J., Ma, K.-F., 1998. Transition from oblique subduction to collision: earthquakes in the southernmost Ryukyu arc-Taiwan region. J. Geophys. Res. 103, 7211–7229.

Karig, D., 1975. Basin genesis in the Philippine Sea. Init. Repts. Deep Sea Drill. Proj. 31, 857–879.

Karig, D.E., 1983. Accreted terranes in the northern part of the Philippine archipelago. Tectonics 2, 211–236.

Lallemand, S.E., Popoff, M., Cadet, J.P., Bader, A.G., Pubellier, M., Rangin, C., Deffontaines, B., 1998. Genetic relations between the central and southern Philippine Trench and the Sangihe Trench. J. Geophys. Res. 103, 933–950.

Lin, J.-Y., Lo, C.-L., 2013. Earthquake-induced crustal gravitational potential energy change in the Philippine Area. J. Asian Earth Sci. 66, 215–223.

McCabe, R., Almasco, J., Diegor, W., 1982. Geologic and paleomagnetic evidence for a possible Miocene collision in western Panay, central Philippines. Geology 10, 325–329.

McCabe, R., Almasco, J.N., Yumul, G., 1985. Terranes of the central Philippines. Tectonostratigraphic terranes of the circum-Pacific region, pp. 421-436.

McCaffrey, R., 1992. Oblique plate convergence, slip vectors, and forearc deformation. J. Geophys. Res. 97, 8905–8915.

Michael, A.J., 1984. Determination of stress from slip data: faults and folds. J. Geophys. Res. 89, 11517–11526.

Pubellier, M., Garcia, F., Loevenbruck, A., Chorowicz, J., 2000. Recent deformation at the junction between the North Luzon block and the Central Philippines from ERS-1 Images. Island Arc 9, 598–610.

Querubin, C.L., Yumul, G.P., 2001. Stratigraphic correlation of the Malusok volcanogenic massive sulfide deposits, Southern Mindanao, Philippines. Resour. Geol. 51, 135–143.

Ramos, N.T., Dimalanta, C.B., Besana, G.M., Tamayo, R.A., Yumul, G.P., Maglambayan, V.B., 2005. Seismotectonic reactions to the arc-continent convergence in central Philippines. Resour. Geol. 55, 199–206.

Rangin, C., Le Pichon, X., Mazzotti, S., Pubellier, M., Chamot-Rooke, N., Aurelio, M., Walpersdorf, A., Quebral, R., 1999. Plate convergence measured by GPS across the Sundaland/Philippine Sea Plate deformed boundary: the Philippines and eastern Indonesia. Geophys. J. Int. 139, 296–316.

Ringenbach, J.C., Pinet, N., Stéphan, J.F., Delteil, J., 1993. Structural variety and tectonic evolution of strike-slip basins related to the Philippine Fault System, northern Luzon, Philippines. Tectonics 12, 187–203.

Sajona, F.G., Bellon, H., Maury, R.C., Pubellier, M., Quebral, R.D., Cotten, J., Bayon, F.E., Pagado, E., Pamatian, P., 1997. Tertiary and quaternary magmatism in Mindanao and Leyte (Philippines): geochronology, geochemistry and tectonic setting. J. Asian Earth Sci. 15, 121–153.

Sandwell, D.T., Smith, W.H.F., 1997. Marine gravity anomaly from Geosat and ERS 1 satellite altimetry. J. Geophys. Res. 102, 10039–10054.

Sandwell, D.T., Müller, R.D., Smith, W.H., Garcia, E., Francis, R., 2014. New global marine gravity model from CryoSat-2 and Jason-1 reveals buried tectonic structure. Science 346, 65–67.

Sherlock, R.L., Barrett, T.J., Lewis, P.D., 2003. Geological setting of the Rapu Rapu gold-rich volcanogenic massive sulfide deposits, Albay Province, Philippines. Mineral. Deposita 38, 813–830.

Simplina-Manahan, J.J., 2004. Source Characterization of the 15 November 1994, Ms 7.1 Mindoro, Philippines Earthquake. AGU Fall Meeting Abstracts.

Tang, Q., Zheng, C., 2013. Crust and upper mantle structure and its tectonic implications in the South China Sea and adjacent regions. J. Asian Earth Sci. 62, 510–525.

Wu, W.-N., Kao, H., Hsu, S.-K., Lo, C.-L., Chen, H.-W., 2010. Spatial variation of the crustal stress field along the Ryukyu-Taiwan-Luzon convergent boundary. J. Geophys. Res. 115, B11401. http://dx.doi.org/10.1029/2009JB007080.

Wessel, P., Smith, W.M.F., 1998. New improved version of generic mapping tools released. EOS Trans. AGU 79, 579.

Wu, W.-N., Hsu, S.-K., Lo, C.-L., Chen, H.-W., Ma, K.-F., 2009. Plate convergence at the westernmost Philippine Sea Plate. Tectonophysics 466, 162–169.

Wu, Y.-M., Hsu, Y.-J., Chang, C.-H., Teng, L.S., Nakamura, M., 2010. Temporal and spatial variation of stress field in Taiwan from 1991 to 2007: Insights from comprehensive first motion focal mechanism catalog. Earth Planet. Sci. Lett. 298, 306–316.

Yu, S.-B., Hsu, Y.-J., Bacolcol, T., Yang, C.-C., Tsai, Y.-C., Solidum, R., 2013. Present-day crustal deformation along the Philippine Fault in Luzon, Philippines. J. Asian Earth Sci. 65, 64–74.

Yumul, G.P., 2007. Westward younging disposition of Philippine ophiolites and its implication for arc evolution. Island Arc 16, 306–317.

Yumul, G.P., Dimalanta, C.B., Tamayo Jr., R.A., Maury, R.C., 2003. Collision, subduction and accretion events in the Philippines: a synthesis. Island Arc 12, 77–91.

Yumul, G.P., Dimalanta, C.B., Tamayo, R.A., 2005. Indenter-tectonics in the Philippines: example from the Palawan microcontinental block-philippine mobile belt collision. Resour. Geol. 55, 189–198.

Yumul, G.P., Dimalanta, C.B., Maglambayan, V.B., Marquez, E.J., 2008. Tectonic setting of a composite terrane: a review of the Philippine island arc system. Geosci. J. 12, 7–17.

Yumul, G.P., Jumawan, F.T., Dimalanta, C.B., 2009a. Geology, geochemistry and chromite mineralization potential of the amnay ophiolitic complex, Mindoro, Philippines. Resour. Geol. 59, 263–281.

Yumul, G.P., Dimalanta, C.B., Marquez, E.J., Queaño, K.L., 2009b. Onland signatures of the Palawan microcontinental block and Philippine mobile belt collision and crustal growth process: a review. J. Asian Earth Sci. 34, 610–623.